Current Opinion in Solid State and Materials Science 16 (2012) 10–22

Contents lists available at ScienceDirect

Current Opinion in Solid State and Materials Science

journal homepage: www.elsevier.com/locate/cossms

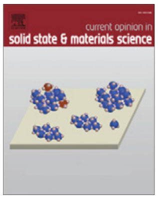

Nanostructural and chemical characterization of supported metal oxide catalysts by aberration corrected analytical electron microscopy

Wu Zhou [a,*], Israel E. Wachs [b], Christopher J. Kiely [a,b,*]

[a] Department of Materials Science and Engineering, Lehigh University, Bethlehem, PA 18015, USA
[b] Department of Chemical Engineering, Lehigh University, Bethlehem, PA 18015, USA

ARTICLE INFO

Article history:
Received 15 March 2011
Accepted 5 June 2011
Available online 22 June 2011

Keywords:
Analytical electron microscopy
STEM
HAADF imaging
EELS
Catalysis
Supported metal oxide catalyst
WO_3
ZrO_2
TiO_2
SiO_2

ABSTRACT

The performance of catalyst materials are usually governed by the precise atomic structure and composition of very specific catalytically active sites. Therefore, structural and chemical characterization at the atomic scale becomes a vital requirement in order to identify any structure–performance relationships existing in heterogeneous catalyst systems. Aberration-corrected scanning transmission electron microscopy (STEM) represents an ideal means to probe the atomic scale structural and chemical information via a combination of various imaging and spectroscopy techniques. In particular, high-angle annular dark-field (HAADF) imaging provides directly interpretable atomic number (Z) contrast information; while X-ray energy dispersive spectroscopy (XEDS) and electron energy-loss spectroscopy (EELS) spectrum imaging can be used to identify the chemical composition and oxidation state. Here we review some applications of aberration-corrected STEM to catalyst research, firstly in the context of supported metal catalysts, which serve as ideal material systems to illustrate the power of these techniques. Then we focus our attention on more recent progress relating to the characterization of supported metal oxide catalysts using aberration-corrected STEM. We demonstrate that it is now possible to directly image supported surface oxide species, study oxide wetting characteristics, identify the catalytic active sites and develop new insights into the structure–activity relationships for complex double supported oxide catalysts. Future possibilities for *in situ* and gentle low voltage electron microscopy studies of oxide-on-oxide materials are also discussed.

1. Introduction

Heterogeneous catalysts are an important research topic owing to their irreplaceable role in chemical and fuel production as well as environmental control. One key aspect in catalysis research is to identify structure–performance relationships, which can help in improving catalytic performance and designing better catalyst materials. It has been well documented that the performance of heterogeneous catalyst materials depends on a variety of parameters including particle size and shape, catalyst surface structure, local composition and chemical bonding, interaction between the surface overlayer/particle and the support materials, and evolution of these key parameters during catalyst synthesis, application and regeneration.

In the characterization of supported metal oxide on metal oxide catalysts, such information has traditionally been acquired using optical spectroscopy techniques (including UV–vis, Raman, and infra-red (IR) spectroscopies) and X-ray techniques (including X-ray diffraction (XRD), small angle X-ray scattering (SAXS), extended X-ray absorption fine structure (EXAFS), X-ray absorption near edge structure (XANES), and X-ray photoelectron spectroscopy (XPS)). For example, UV–vis spectroscopy can provide information on the electronic structure of the surface oxide domains [1,2], and can be used to monitor the oxidation state change during reaction [3]. Raman spectroscopy is well known as a sensitive technique to discriminate between multiple molecular structures that may be present in the sample volume [3–5]. IR spectroscopy is widely adopted in the identification the surface species at the molecular level [4,5]. These optical spectroscopy methods often provide important information that is difficult to access from other techniques. Similarly, XPS can routinely provide highly sensitive surface compositional and chemical state analysis, and local atomic structure and bonding information can be easily accessed using EXAFS [5]. Characterization studies using these spectroscopic techniques have provided many insights into the structure–activity relationships for supported metal oxide catalyst

---

* Corresponding authors. Addresses: Department of Physics & Astronomy, Vanderbilt University, Nashville, TN 37235, USA (W. Zhou). Department of Materials Science and Engineering, Lehigh University, Bethlehem, PA 18015, USA(C.J. Kiely).

E-mail addresses: wu.zhou@vanderbilt.edu (W. Zhou), chk5@lehigh.edu (C.J. Kiely).

1359-0286/$ - see front matter © 2011 Elsevier Ltd. All rights reserved.
doi:10.1016/j.cossms.2011.06.001

systems, especially when they are combined with *in situ* reaction cells, in which the catalytic materials are exposed to an environment similar to that experienced under normal operating conditions [5].

However, there is one significant drawback with all the techniques mentioned above since they can only provide spatially averaged information over a relatively large surface area of the catalyst material under investigation (on the order of ~micron^2). It has been shown for many highly active heterogeneous catalyst systems that a variety of different surface structures can co-exist, with sizes ranging from single atoms to 10 nm particles, and sometimes the catalytic important structure may only constitute a minor part of the catalyst material. For example, supported WO_3/ZrO_2 acid catalysts contain Zr-containing WO_3 clusters that are the catalytic active sites and may represent only a small fraction of the total tungsten oxide present in the catalyst [3]. Similarly, Herzing et al. showed that ~0.5 nm bilayer Au clusters in supported Au/FeO_x catalyst system are the most active species for CO oxidation at low temperature, which, however, only represents ~1 wt.% of the total Au loading in the catalyst material [6]. Therefore, in order to obtain new insights into the structure of the catalytically active species, the structure–performance relationship, and the identification of other factors that may affect the catalyst properties, the conventional optical and X-ray spectroscopy methods must be complemented with local structural and compositional analysis techniques that have a spatial resolution on the nm or atomic scale. Recent developments in aberration-corrected electron optics [7–9] have pushed the spatial resolution in a (scanning) transmission electron microscope ((S)TEM) down into the sub-Angstrom regime, providing an ideal platform to carry out direct imaging and chemical analysis of the local structure in heterogeneous supported catalysts.

Electron microscopy is now well recognized as an indispensable tool in catalyst research, especially for the study of supported metal catalysts [10], supported metal oxide [11] and bulk metal oxide catalysts [12]. TEM-based techniques, such as bright field (BF) imaging, high resolution TEM (HRTEM) imaging, energy-filtered TEM (EF-TEM) and electron diffraction, have been frequently used to provide information on the particle shape and size distribution, exposed facet planes, active phase identification, particle/support epitaxy and elemental distribution. In particular, HRTEM imaging (also known as phase contrast imaging) can provide useful real-space structural information at the atomic level. When combined with theoretical simulation and aberration-corrected techniques, either via the use of an imaging aberration corrector [13] or by through-focus exit wave reconstruction, detailed surface atomic structure information can be obtained from HRTEM imaging [14,15]. However, the phase contrast imaging technique is very sensitive to sample thickness, image defocus, beam tilt, and numerous other experimental parameters. Furthermore, quantitative image simulation is often required if detailed structural information from specific features (*e.g.* surface reconstruction analysis) needs to be extracted from HRTEM experiments.

As an alternative to these TEM-based methods, there are a host of STEM-based analytical electron microscopy (AEM) techniques, in which a small focused coherent electron beam is scanned across the sample in a raster. STEM-AEM is becoming more and more popular in catalyst research, especially for the structural and chemical characterization of supported metal catalysts in which heavier metal components are dispersed onto low atomic number (Z) supports [10]. A rich variety of signals can be generated via electron-sample interactions and be collected simultaneously as schematically illustrated in Fig. 1. For example, characteristic X-ray signals can be used for chemical analysis, and post-specimen electron signals can be collected by different detectors to form images or/and electron energy loss spectra. By choosing different collection angle ranges, bright field (BF), annular bright field (ABF [16]), and annular dark-field (ADF) STEM images can be collected. In particular, by changing the excitation of the post specimen lenses and using an ADF detector having an inner collection angle greater than 50 mrads, a high-angle annular dark-field (HAADF) image can be formed. The signal used in HAADF images are mainly Rutherford scattered electrons which are strongly dependent upon the square of atomic number ($Z^{1.5-1.8}$) of the atoms present in the area being imaged [17,18]. Thus, Z-contrast information can be directly obtained from STEM-HAADF images. Moreover, the inelastic scattered electrons can be collected using an electron energy-loss (EEL) spectrometer as a function of probe position, providing compositional information with atomic resolution [19].

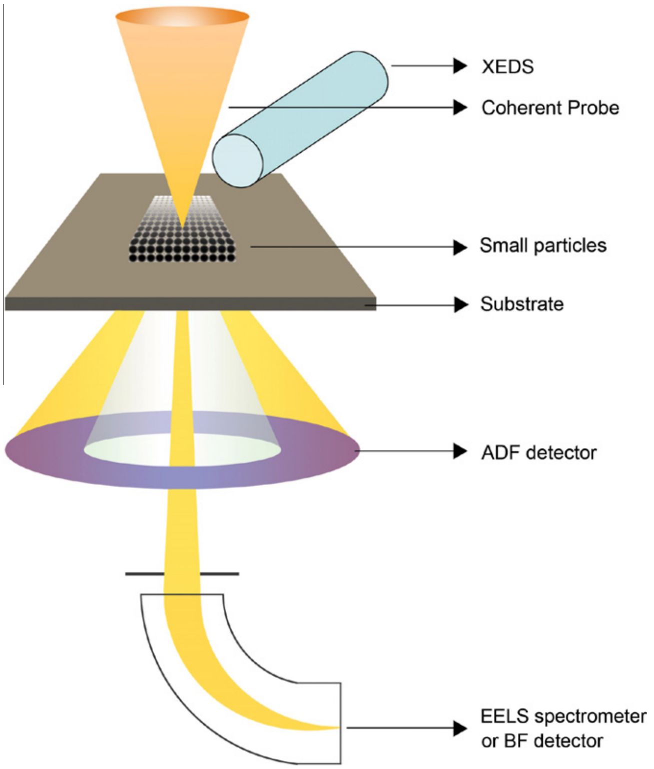

Fig. 1. Schematic diagram illustrating the various signals generated inside a scanning transmission electron microscope (STEM) that can be used for imaging and nanoanalysis.

Compared to the application of such electron microscopy techniques in the study of supported metal catalysts [9,10,20], there is relatively little corresponding activity in the area of supported metal oxide catalysts. In this article, we will specifically focus on recent progress in the study of supported metal oxide catalysts using aberration-corrected STEM imaging and chemical analysis techniques. A brief review of the important structural and chemical analysis techniques accessible in STEM and their applications to the study of supported metal catalysts will first be presented. This will be followed by a few case studies from our own research on supported metal oxide catalysts where aberration-corrected STEM has been used to directly image the surface structure, identify the catalytic active sites and reveal new insights into the structure–activity relationships that for supported oxide catalyst systems. A general discussion of future perspectives and challenges will be presented in the last section of this article.

1.1. STEM-HAADF imaging of supported metal catalysts

The development of the probe aberration corrector has provided STEM-HAADF imaging with an unprecedented ability to provide Z-contrast information with sub-Å spatial resolution [22] and single atom sensitivity [23,24]. It is well known that the electron probe size and thus the spatial resolution of imaging and chemical analysis in STEM is mainly limited by the third-order spherical aberration coefficient (C_s), which is unavoidable for conventional rotationally symmetric magnetic lenses. This limitation can be overcome by using a series of multipole lenses that break the rotational symmetry as proposed by Scherzer more than 60 years ago [25]. A significant increase in beam current, while retaining or reducing the probe size, can be achieved using C_s-corrector technology, which ensures a high signal-to-noise ratio in the resulting high resolution STEM images and chemical analyses. A simulation of the intensity distribution for an electron probe before and after spherical aberration correction is shown in Fig. 2.

For most aberration-corrected (S)TEM instruments, a 1.36Å spatial resolution can be routinely achieved for HAADF imaging; while a 0.5Å spatial resolution has been recently demonstrated on several instruments with the latest lens designs [22,26,27]. The ability to provide single atom detection with high spatial resolution and signal-to-noise ratio has led to aberration corrected HAADF imaging being used in many successful applications for the structural study of supported metal catalysts such as La/Al_2O_3 [28], Au/TiO_2 [9], and Au/FeO_x [6]. For example, in a recent study Herzing et al. demonstrated that HAADF imaging can be used to image *all* the surface species, from large Au nanoparticles to single surface Au atoms, present in the Au/FeO_x catalyst system (Fig. 3) [6]. The *co-existence* of different supported structures is a common situation in many practical catalyst systems, and the high resolving power of the HAADF imaging technique can ensure that all the fine structural information can be clearly captured. Thus, a population distribution of all the different Au species present can be satisfactorily deduced by analyzing a large of number of images obtained from the samples. By correlating the catalytic performance with the distribution of different Au species in a systematic set of Au/FeO_x catalysts (Fig. 3C), Herzing et al. were able to identify sub-nm bi-layer Au clusters (Fig. 3B) as the most catalytically active species for low temperature CO oxidation [6]. This particular identification was a formidable achievement as these sub-nm bi-layer Au clusters only constituted a very small fraction (<1%) of the total Au loading, which could well be missed or considered as being insignificant using other 'averaging' characterization techniques.

An enhanced signal-to-noise ratio in HAADF imaging is also a benefit gained from spherical aberration correction, which makes it possible, in some instances, to determine the chemical identities of specific atoms or atomic columns/layers, since the HAADF signal is proportional to $Z^{1.5-1.8}$ Ref. [29]. As shown in Fig. 4A, single Pt and Ru atoms within a bimetallic cluster on an Al_2O_3 support can be clearly distinguished by their different HAADF image intensities, which is almost impossible to discern from conventional STEM-EELS or STEM-XEDS analysis due to the high mobility of the atoms on the free surface and the low EELS/XEDS signal from individual atoms. Similarly, for bi-metallic nanoparticles such as the Au–Pd particle shown in Fig. 4B, the distinctive intensity variation across the particle diameter indicates that this is an Au–Pd nanoparticle with a Au-rich core and Pd-rich shell. This type of chemical information can be obtained straightforwardly from the HAADF image without performing time consuming STEM-EELS or STEM-XEDS mapping experiments.

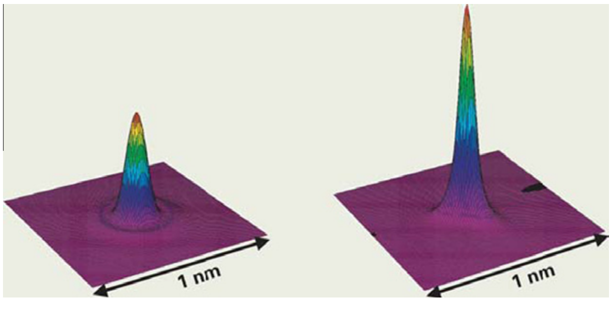

Fig. 2. The simulated intensity distributions of an electron probe of Lehigh's JEOL 2200FS (S)TEM before (left) and after (right) C_s correction. Reprinted from Ref. [21].

It should be noted that without image simulation, chemical information relating to the samples can only be qualitatively obtained in some favorable cases by analyzing the HAADF image contrast. In order to "squeeze" even more useful structural and chemical information from such experimental HAADF micrographs, image simulation becomes essential since the intensity of the HAADF image can be affected by many factors, *e.g.* the height position of the single atoms [28], the number of atoms along the beam direction [23,31], the instrument settings [32], and the specimen tilt angles [33]. For example, Wang et al. [28] have shown that La atoms adsorbed on the bottom surface of a γ-Al_2O_3 flake (*i.e.* the exit plane of the electron beam) exhibited a higher image intensity as compared with those La atoms adsorbed on the top surface (*i.e.* the entrance plane of the electron beam) as shown in Fig. 5. Recent developments in STEM-HAADF image simulation methodology can now match the simulated image intensity quantitatively with the experimental image intensity [34], which in principle can help to extract both compositional and structural information from such atomically resolved HAADF images.

The distribution and configuration of supported metal atoms on an oxide support surface experimentally obtained from HAADF imaging can serve as useful input data for DFT calculations, which can in turn help theorists to understand the surface structure and metal-support interactions in supported metal catalysts [28,35]. Such DFT calculations can in turn be used to judge whether or not the structural model proposed for an image simulation is energetically favorable.

Another important benefit of the aberration corrected STEM instrument is that a larger probe forming aperture can be used, which dramatically reduces the depth of focus (Δz), following a $\Delta z \approx \lambda/\theta^2$ dependency, where θ is the illumination semi-angle as defined by the probe forming aperture. This potentially allows for three-dimensional reconstruction by depth sectioning of individual heavy metal atoms or particles within the support material/matrix, whereby a through-focal HAADF image series is recorded in a similar manner to that used in optical confocal microscopy [36,37]. Early examples of this technique include the identification of the relative positions of Pt–Au nanoparticles on TiO_2 support materials by Borisevich et al. [36] and determining the location of individual Hf atoms in the SiO_2 passivating layer in a semiconductor device [38]. As an alternative to depth-sectioning, 3D imaging in catalyst systems can also be achieved by STEM-HAADF electron tomography. This is an important technique that is still under active development, and some recent advances in this area have been reviewed elsewhere [20,39].

1.2. Spectrum imaging with EELS and/or XEDS for supported metal catalysts

The elemental distribution in the materials can be obtained by combining the imaging and analytical capability of a STEM, in a technique which is known as spectrum imaging (SI) [40–43]. In SI, a full spectrum (either EELS or XEDS) is collected at and registered to each pixel of the digital image. The dataset acquired constitutes a 3D data cube with the STEM image in the X–Y plane and the EELS/XEDS spectra in the Z direction. Elemental maps can be obtained by slicing the data cube at a specific energy plane in the Z direction and adding/subtracting different energy planes for summation or background subtraction.

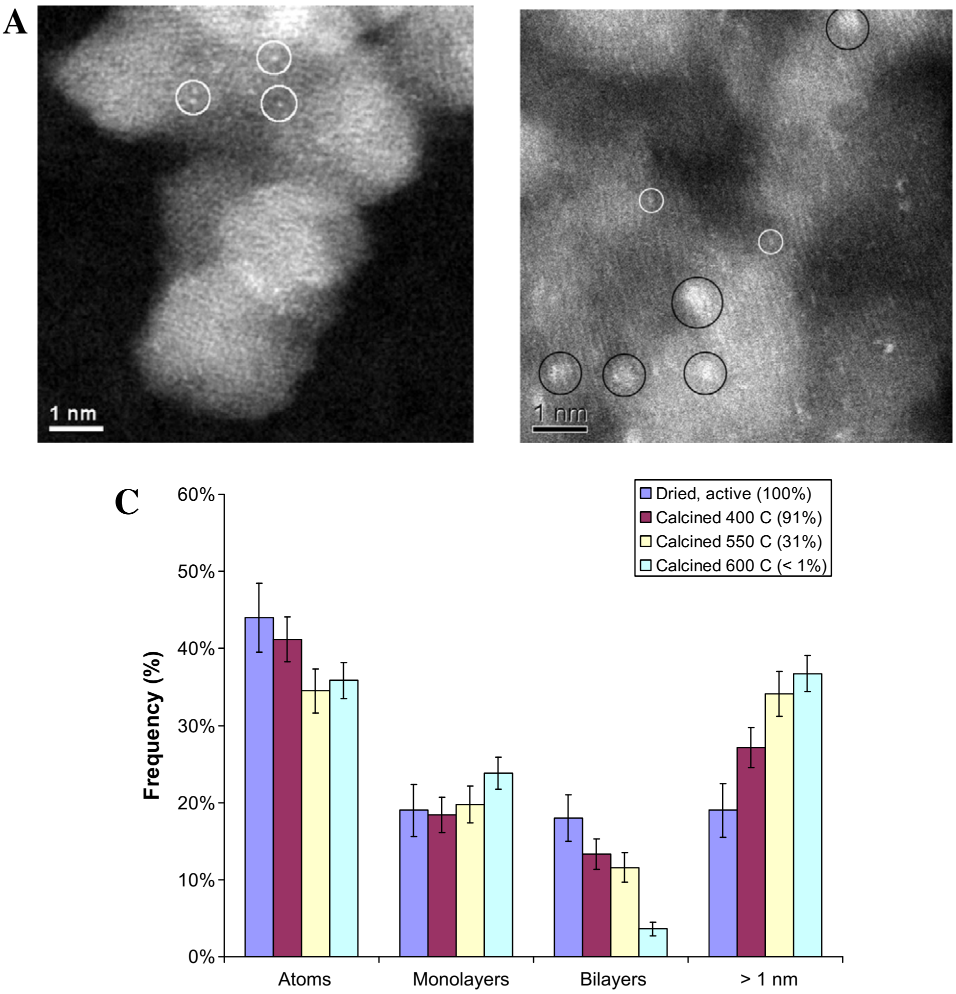

Fig. 3. (A and B) Representative high resolution STEM-HAADF images of (A) an inactive and (B) an active Au/FeO$_x$ catalyst synthesized by very similar methods. The white circles highlight the presence of isolated Au atoms, while the black circles indicate sub-nm Au clusters that only present in the highly active catalyst; (C) Relative populations of different supported Au species as a function of catalyst calcination temperature and measured CO conversion. Reprinted from Ref. [6] with permission from AAAS.

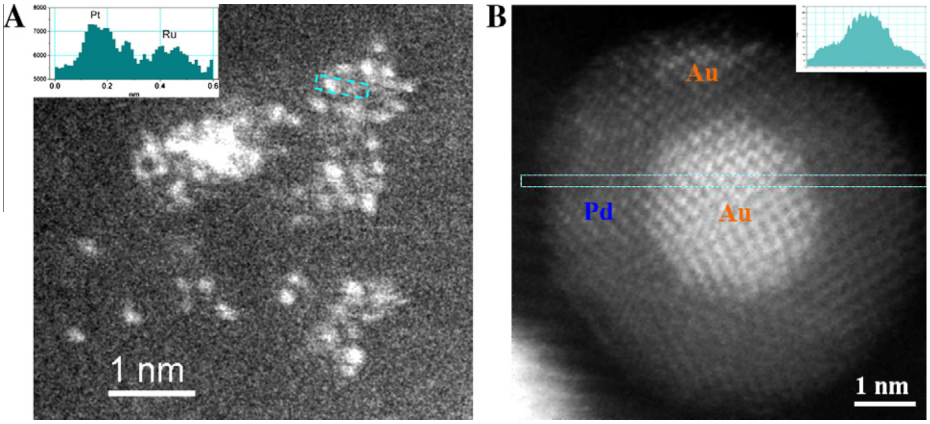

Fig. 4. Aberration-corrected STEM-HAADF images from (A) Pt–Ru/γ-Al$_2$O$_3$ (Reprinted from Ref. [30], by permission of the Cambridge University Press.) and (B) Au–Pd/TiO$_2$ catalysts (sample courtesy of Dr. N. Dimitratos and Prof. G. J. Hutchings, Cardiff University, UK.). *Inserts:* Intensity line profiles from the samples as indicated on the images.

Aberration correction has not only significantly increased the spatial resolution of STEM spectrum imaging, but also drastically improved the detection sensitivity [44,45] by increasing the current density in the small electron probe. When combined with advanced data processing software, *e.g.* multivariate statistical analysis (MSA) [46] or principal component analysis (PCA) [47] which aim to remove random noise from the spectrum images, minor compositional features can also be satisfactorily extracted from the STEM-SI due to the enhanced signal-to-noise ratio.

Several elegant demonstrations of the application of STEM-XEDS SI in the chemical analysis of supported bimetallic catalysts have been reported by Herzing et al. [42,48,49]. Combining

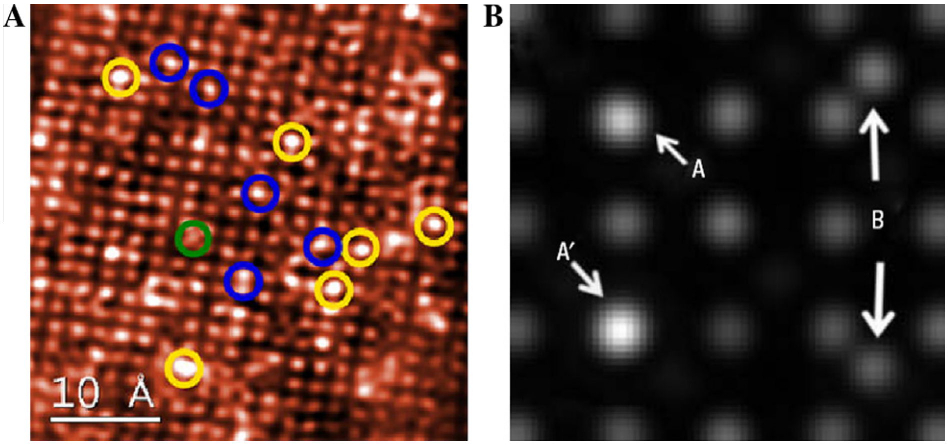

Fig. 5. Experimental and simulated STEM-HAADF images of La atoms on a γ-Al_2O_3 flake in the [100] zone axis projection. Image simulations indicate that the La atoms on the bottom surface are brightest (yellow & A'), while those on the top surface are less bright (blue & A). Interstitial La atoms display the weakest contrast (green & B). Reprinted by permission from Macmillan Publishers Ltd.: [Nature Materials] (Ref. [28]), copyright (2004).

aberration corrected STEM spectrum imaging with multivariate statistical analysis (MSA), Herzing et al. have been able to determine (i) core–shell morphology development in bimetallic nanoparticles; (ii) particle size-composition relationships in supported Au–Pd catalysts; (iii) the detection of impurity elements at trace levels (<1 at.%); and (iv) mapping the spatial distribution of highly dispersed metal species on oxide supports [42,48,49]. They found that the composition of Au–Pd nanoparticles prepared by co-precipitation techniques varied with size in a systematic way, such that the largest particles were Au-rich while the smallest particles tended to be Pd-rich [42] as shown in Fig. 6, suggesting possible tuning of the bimetallic composition and the resultant catalytic activity by controlling the particle size [50].

High sensitivity XEDS mapping with a detection limit as low as 3 atoms/nm^2 has been demonstrated by Watanabe et al. [45] using the aberration corrected VG HB603 STEM at Lehigh. Atomic resolution 2-D chemical imaging of composition and bonding in perovskite multilayer thin film materials using EELS-SI in an aberration corrected UltraSTEM have also been recently demonstrated by Muller et al. [19]. It should be noted that for spectrum imaging with high resolution and single atom sensitivity, a small electron probe with high current density on a C_s-corrected instrument is essential, but this is now possible with recent advances in electron optics. However, it should be also be recognized that the robustness of the material to electron beam irradiation damage under the prolonged high energy electron bombardment required for SI acquisition will always be a major limitation for high resolution spectrum imaging.

1.3. Summary of the very limited previous AEM work on supported oxide-on-oxide catalysts

As compared to supported metal catalysts, only a very limited number of electron microscopy studies on supported

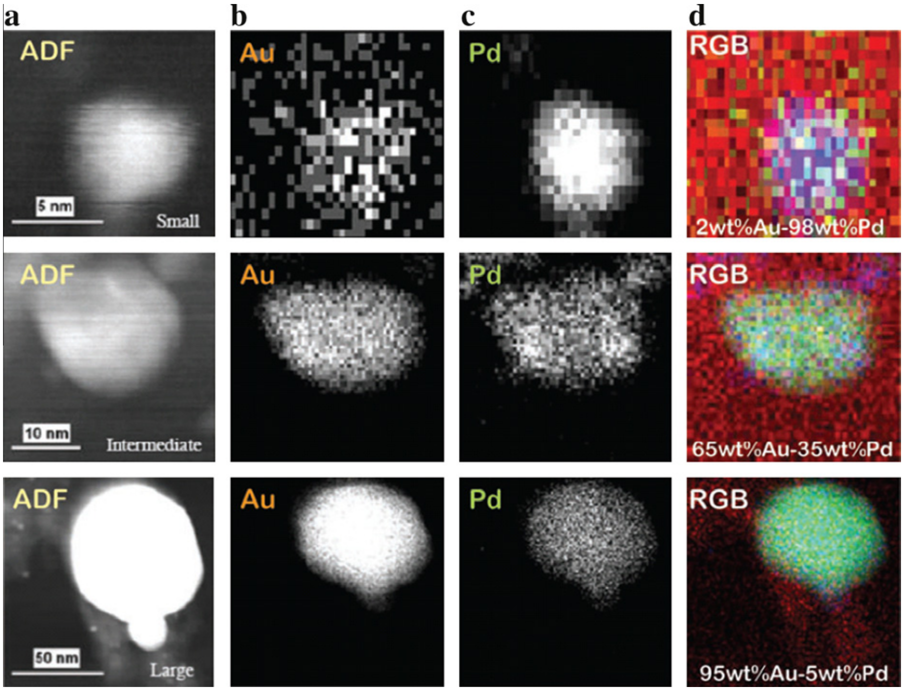

Fig. 6. STEM-XEDS spectrum images showing the relationship between the particle size and composition in Au–Pd nanoparticles in a Au–Pd/C catalyst. (a) ADF image, (b) Au L_α XEDS map, (c) Pd L_α XEDS map and (d) RGB overlays [Red – C: Green – Au: Blue – Pd] from small (row 1), intermediate size (row 2) and large (row 3) Au–Pd particles. Reprinted from Ref. [42] by permission of The Royal Society of Chemistry.

oxide-on-oxide catalysts have been reported to date. Burrows and Kiely used HRTEM to study the surface WO_x structure on a monolayer WO_3/TiO_2 supported catalyst [51], and they were able to observe the polytungstate domains on the TiO_2 surface, which had a tendency to change into WO_x clusters due to electron beam irradiation damage. (Since electron beam damage in such samples is an important issue in its own right, it will be discussed in more detail in Section 3.2.) The HRTEM approach was later extended to the study of other oxide-on-oxide catalysts [3,12,52–56]. However, the application of HRTEM to characterize the surface structure of supported metal oxide catalysts is hindered by image delocalization effects in non-aberration-corrected FEG-TEM instruments and the formation of complex sub-monolayer catalytic active species on the support surface [3,11], which generate little or no contrast in the phase contrast image. So far, single atom detection on an oxide support surface has not been reported using the HRTEM technique. There were also some attempts to employ EF-TEM imaging to study the relative distribution of W and Zr species in a co-precipitated WO_3/ZrO_2 catalyst as a function of calcination temperature [53,54]. However, this method failed to provide a reliable W map in this specific case due to a severe overlap of Zr and W signals in the low-loss regime [57].

Few STEM imaging studies have been reported on oxide-on-oxide catalysts due to the technical difficulties arising from (i) having a very high dispersion of the overlayer oxide on the support and (ii) having a relatively small Z difference between the two cationic components in many oxide-on-oxide catalyst systems. The most relevant early publication was reported by Borisevich et al. [58] for supported Cr_2O_3/Al_2O_3 catalysts. However, the low contrast levels in the HAADF images resulted in insufficient statistics to discriminate single Cr atoms on the Al_2O_3 surface [58]. Cortes-Jácome et al. [59] used STEM-HAADF imaging and XEDS analysis to identify the presence of WO_x clusters $\sim$ 1 nm in size on a TiO_2 support. However, they were limited by the spatial resolution of their non-aberration-corrected instrument, and atomic resolution imaging was not achieved. As a result, the very smallest surface WO_x species present (*i.e.* mono- and poly-tungstate species which will be described in more detail in the next section) were not directly resolved in their study, which consequently prevented them from establishing an unambiguous relationship between the surface WO_x structure and the catalytic properties.

It should be mentioned that the characterization of oxide–oxide interfaces or multilayer structures has been one the mainstays of electron microscopy for many years [60]. The oxide components in these oxide–oxide systems often have well-defined crystalline structures, and are rather robust under the electron beam. Due to their high structural stability, atomic resolution imaging and chemical mapping experiments (both of which favor a high probe current and long acquisition times) can now be routinely performed on these systems [19] using aberration-corrected STEM. However, the oxide-on-oxide catalysts, which are the focus of this article, are distinctly different from these oxide–oxide multilayer structures. In particular, the very high dispersion of the oxide overlayer on the oxide catalyst supports implies that the surface oxide species are prone to have a higher surface mobility under the stimulus of the electron beam, and that high probe currents and long acquisition times should be avoided during STEM experiments. This potential structural instability, thus, makes it much more challenging type of system for electron microscopy characterization as compared with the more durable oxide–oxide multilayer structures.

In the following section, we will show through three case studies that aberration-corrected STEM provides a unique opportunity to push the limit of structural and compositional characterization of supported oxide-on-oxide catalysts at the atomic scale. This ability now permits us obtain important new insights into the structure–activity relationships for such complex catalyst systems containing multiple catalytic active site structures. Some further technical discussion about strategies for minimizing the potential of electron beam damage to the samples will be presented in Section 3.2 following the case studies.

2. Case studies for oxide-on-oxide catalyst systems

2.1. Identifying the nature of catalytic active sites on supported WO_3/ZrO_2 solid acid catalysts using STEM-HAADF imaging

Tungsten oxide supported on zirconia has been well recognized as a strong solid acid catalyst for the isomerization of light (C_4 to C_8) alkanes at low temperature, in which naturally abundant straight-chain alkanes are converted into branched alkanes for the production of higher quality gasoline and other industrially important feedstock. This catalyst has a promising future for practical industrial applications owing to their enhanced thermal and environmental stabilities. Over the past two decades, an extensive variety of catalyst synthesis methods, characterization techniques and catalytic performance testing studies have been applied to this catalyst system in an attempt to establish a relationship between the synthesis method, catalyst structure and catalytic performance. Previous studies suggest that the catalytic activity of tungstated zirconia catalysts depends on the nanostructure of the surface WO_x species present, which can include mono-tungstate, poly-tungstate, WO_x clusters, and 'bulk' WO_3 crystals (Fig. 7) [3,11]. However, much remains to be learned about this particular catalyst system. In particular, identification of the precise nature of the most catalytically active tungstate species was, until very recently, an issue of ongoing debate due to a lack of unambiguous imaging of these surface WO_x entities on ZrO_2. Therefore, detailed experimental evidence at the atomic scale for the presence of the various tungsten oxide species on the ZrO_2 surface becomes a key criterion for identifying pertinent structure–activity relationships.

Using aberration corrected STEM-HAADF imaging, we reported the first direct imaging of all the surface WO_x entities on the ZrO_2 support, which enabled us to identify the key catalytic active site and provide new insights into the structure–activity relationships for the supported WO_3/ZrO_2 catalyst system [11]. The fundamental structural information derived from this electron microscopy study has also subsequently led to the rational design of a superior new catalyst [11].

The study was performed on a systematic set of supported WO_3/ZrO_2 catalysts having different surface tungstate loadings and catalytic activities, which are summarized in Fig. 8. For the low activity sample, the WO_x was found to be highly dispersed on the ZrO_2 surface mainly as mono- and poly-tungstate species which have single atomic-layer thickness (Fig. 8A). The existence of these surface species have long been proposed in the literature, however, this is the first time that they were directly imaged and identified. The highly dispersed nature of these two-dimensional surface entities accounts for the structural characterization difficulties encountered in previous studies, as it creates only a very low image contrast in conventional HRTEM images. The high activity samples, however, featured additional numerous disordered WO_x clusters $\sim$0.8–1.0 nm in size (Fig. 8B), *co-existing* with the mono- and poly-tungstate species. Determining the composition of such small clusters would be almost impossible using STEM-XEDS/EELS or X-ray techniques, however, the Z-contrast information contained in the STEM-HAADF images are very useful in this respect. As shown in Fig. 9, contrast variations can often be observed in HAADF images from these $\sim$1 nm clusters when viewed in profile, which was identified via imaging simulation and

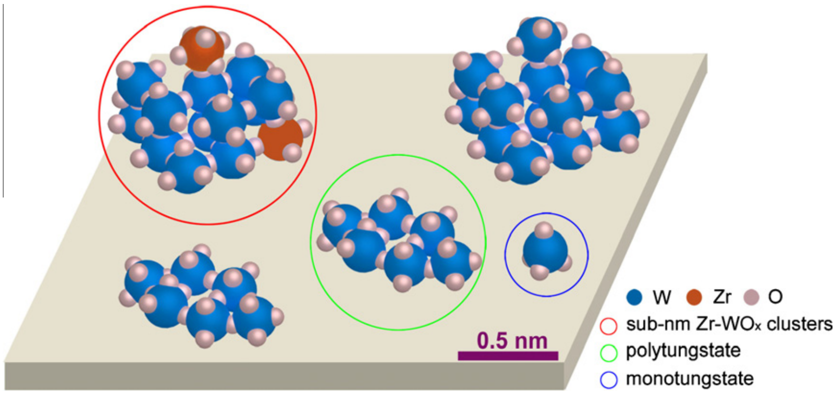

Fig. 7. Schematic representation of mono-tungstate, two-dimensional poly-tungstate, and three-dimensional WO_x clusters supported on ZrO_2 surfaces.

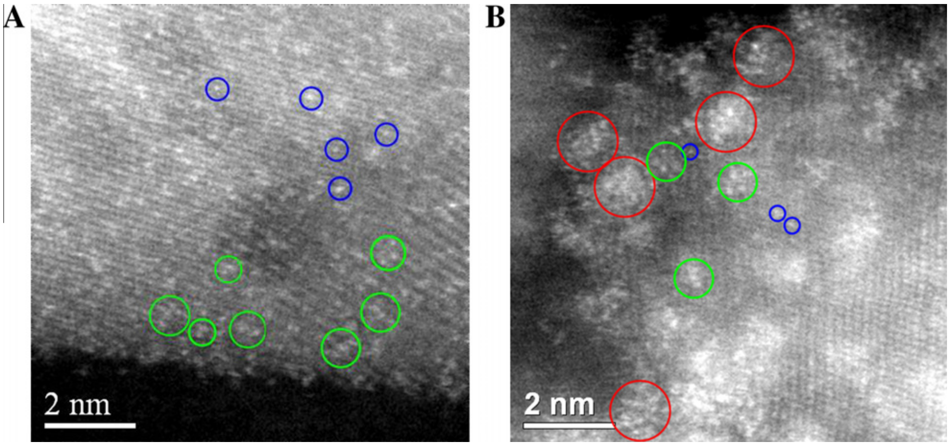

Fig. 8. Representative STEM-HAADF images of supported WO_3/ZrO_2 catalysts. (A) A catalyst with low catalytic activity and (B) a highly active catalyst. The blue circles highlight the presence of single W atoms corresponding to surface mono-tungstate species, and the green circles indicate surface poly-tungstate species with several W atoms linked by oxygen bridging bonds. The red circles highlight Zr–WO_x mixed oxide clusters with diameter ~0.8–1 nm. These latter clusters were only found in the highly active catalyst samples having a WO_x surface density above monolayer coverage, and are identified as the most catalytic active species [11]. Reprinted from Ref. [11].

complementary *in situ* Raman spectroscopy studies to originate from an intermixing of occasional Zr cations within the WO_x clusters [3,11,57]. The ability to capture all of the surface tungstate species present in a systematic set of samples displaying a variety of catalytic activity allowed us to draw a direct correlation between the surface tungstate structure and the catalytic performance. Using this approach we unequivocally identified that these ~1 nm disordered Zr–WO_x mixed oxide clusters represent the most catalytic active species in the supported WO_3/ZrO_2 catalyst system [11,61].

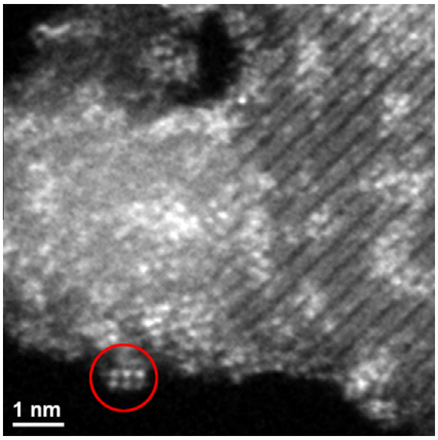

Fig. 9. STEM-HAADF image of a highly active supported WO_3/ZrO_2 catalyst. The red circle highlights a mixed Zr–WO_x cluster in profile view, in which distinct contrast variations at neighboring atomic positions are clearly visible.

The identification of these mixed oxide Zr–WO_x clusters as the catalytic active site provides a new view for supported oxide catalyst research and suggests new directions for the rational design of advanced catalysts with enhanced performance [20]. For instance, we showed that by co-impregnation of amorphous ZrO_x and WO_x precursors onto a crystalline ZrO_2 support, highly active Zr–WO_x clusters can form via thermal-activated surface diffusion, and the catalytic activity can be drastically increased by two orders of magnitude [11].

2.2. Revealing the wetting interactions between different oxide materials using STEM-HAADF imaging

In many oxide-on-oxide catalysts, the catalytic performance depends on the precise surface structure of the active oxide component, which to a large extent is controlled by the interaction between the two oxide components. Here, we use the term “wetting interaction” to qualitatively describe the dispersion of an active oxide on a support surface. A fundamental understanding of the wetting interactions between different oxides is important for the rational design of new oxide-on-oxide catalysts with specific surface structures.

We employed aberration-corrected STEM-HAADF imaging to investigate the wetting interaction between different oxides [11]. Fig. 10 shows representative HAADF images of WO_x supported on several difference oxides: namely ZrO_2, TiO_2 and SiO_2. The distribution and preferred structure of the surface tungstate species are seen to be very different depending on which oxide support is used. On both ZrO_2 and TiO_2 supports, WO_x tends to be atomically dispersed (*i.e.* mono- and poly-tungstate species dominate at low WO_3 loading); whereas on an amorphous SiO_2 support, WO_x clusters about 1 nm in size are the preferred tungstate morphology. This is a direct indication that tungstate species tend to bond more strongly with ZrO_2 and TiO_2 supports than with the SiO_2 support. Furthermore, it was noted that W atoms in the mono-tungstate species tend to adsorb directly above the Zr or Ti support atom columns as shown in Figs. 10A and B, which also suggests that there is a strong propensity for bonding between the surface WO_x species and the crystalline ZrO_2 or TiO_2 support. Different wetting behaviors were also observed on the SiO_2 support material when the overlayer species are different (*i.e.* WO_x and BaO – see Figs. 10 C and D). BaO species were found to form large two-dimensional network structures with individual Ba cations clearly visible on the SiO_2 surface, whereas as ~1 nm 3D clusters were formed by WO_x, indicating a relatively weaker wetting interaction between WO_x and SiO_2. The different wetting interactions visualized through such HAADF images, in principle, could allow one to tailor the structure of the active oxide component by modifying the surface of the primary oxide support material with another metal oxide component, and consequently control the catalytic performance. An example of this catalyst design strategy will be described in the next section.

2.3. New insights into the structure–activity relationships in double-supported $WO_3/TiO_2/SiO_2$ solid acid catalysts

It is clear that STEM-HAADF imaging can effectively provide surface structural information at the atomic scale for a wide variety of 'simple' supported metal oxide catalyst systems. However, many specially designed catalysts, which aim to tailor the catalytic performance, can consist of much more complex nanostructures. An example of such a system are double-supported $WO_3/TiO_2/SiO_2$ catalysts [62,63], in which a high surface area oxide support material (SiO_2) is modified by the presence of a second metal oxide surface species (TiO_2) added to control the distribution and activity of a third active oxide component (WO_3). These complex nanostructures represent a significant challenge in terms of structural characterization, and using STEM-HAADF imaging alone is usually not sufficient to provide the structural and compositional information needed to fully characterize the systems.

In a recent study, we have employed a combination of aberration corrected AEM techniques to characterize a systematic set of double-supported $WO_3/TiO_2/SiO_2$ catalysts [63]. The various oxide components in these double-supported oxide catalysts could be effectively visualized using complementary aberration-corrected HAADF and STEM-BF imaging. Furthermore, when combined with simultaneous chemical analysis by STEM-EELS and XEDS, it was possible to map out the relative spatial distribution of all the supported metal oxides within the $WO_3/TiO_2/SiO_2$ catalysts.

The results obtained from two representative catalyst samples are summarized in Fig. 11. HAADF imaging (Figs. 11A and C) can be reliably used to locate the distribution and discriminate structural details of the active surface WO_x species owing to the high

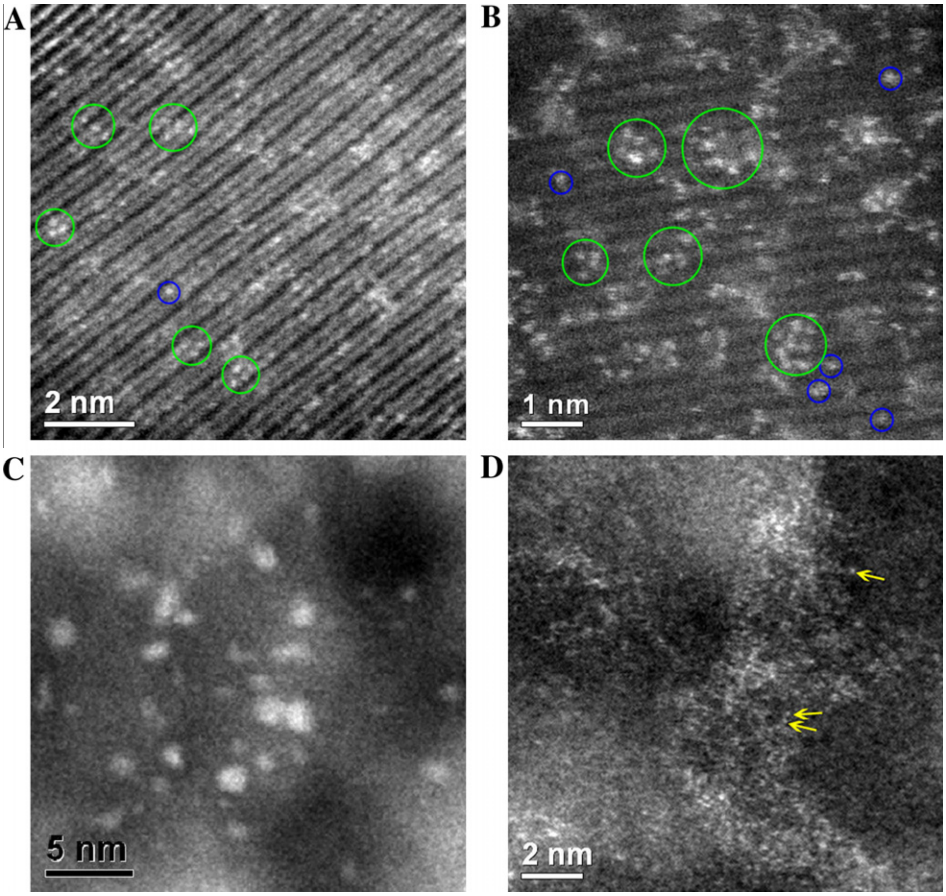

Fig. 10. Aberration-corrected STEM-HAADF images of several supported oxide-on-oxide catalyst systems: (a) a 5 wt% WO_3/ZrO_2 catalyst; (b) a 7 wt% WO_3/TiO_2 catalyst; (c) a 5 wt% WO_3/SiO_2 catalyst; and (d) a 5 wt% BaO/SiO_2 catalyst. All samples were synthesized via standard incipient–wetness impregnation methods followed by a high temperature calcination treatment in air. Reprinted from Ref. [11].

atomic number of W relative to the support. However, information regarding the distribution and structure of the intermediate TiO_x species are absent from the HAADF signal due to the relatively small average atomic number difference between TiO_2 and SiO_2. In contrast, the position and structure of crystalline TiO_2 domains on SiO_2 can be easily identified from the corresponding BF-STEM signal (Fig. 11B) via phase contrast, a method which is often overlooked in the study of supported catalysts. Correlating the HAADF and BF-STEM images, thus, allows us to determine the spatial distribution of the WO_x species with respect to the crystalline TiO_2 component. The possible presence of any non-crystalline TiO_x components on the SiO_2 surface was investigated by STEM-EELS analysis.

Important structural information can often be missed when using just a single imaging or analysis technique, however, an interesting phenomenon was observed when multiple signals were collected simultaneously from these double supported catalysts. By comparing Figs. 11A and B, one can notice that at high TiO_2 loading (30% TiO_2), the WO_x species are preferentially anchored to the crystalline TiO_x rafts as mono-tungstate and poly-tungstate species (as highlighted by red circles in the figures). Moreover, some WO_x species were also found to be atomically dispersed on *non-crystalline* TiO_x areas as evidenced by the presence of a Ti L-edge in EELS analysis and the absence of TiO_2 lattice fringes BF-STEM image from the region delineated by the blue square in Fig. 11B. In contrast, at lower TiO_2 loadings (*i.e.* 5% TiO_2), where TiO_x presents itself solely as amorphous rafts, ~1 nm WO_x clusters were found to be the dominant tungstate structure (Fig. 11C). STEM-EELS spectrum imaging (Fig. 11D) further revealed that the spatial distribution of WO_x clusters (in green) correlates well with the disordered TiO_x rafts (in red), confirming the close association of these two oxide components in this sample.

The combination of aberration-corrected STEM imaging and chemical analysis techniques provide us a new view of the surface WO_x structure and distribution in these double-supported catalysts, *i.e.* at high TiO_2 loading, the WO_x is primarily present as highly dispersed mono- and polytungstate species on larger crystalline TiO_2 domains, while at low TiO_2 loading, ~1 nm WO_x clusters become the dominant structure associated with smaller TiO_x rafts. By correlating this structural information with catalytic testing and electronic structure studies (by UV–vis spectroscopy), the latter nanostructure was identified as being the most beneficial for achieving the best catalytic performance in this double supported catalyst system [63]. Given the structural complexity associated with many high-performance catalysts, we believe that this combined STEM imaging and chemical analysis approach, supplemented by invaluable complementary *in situ* optical spectroscopy techniques, will play an important role in understanding the catalytic behavior of this general class of supported oxide-on-oxide catalyst materials.

3. Future perspectives

As briefly reviewed above, aberration-corrected electron microscopy is now well recognized as a very powerful tool in catalyst research. The rapid development of new instrumentation and

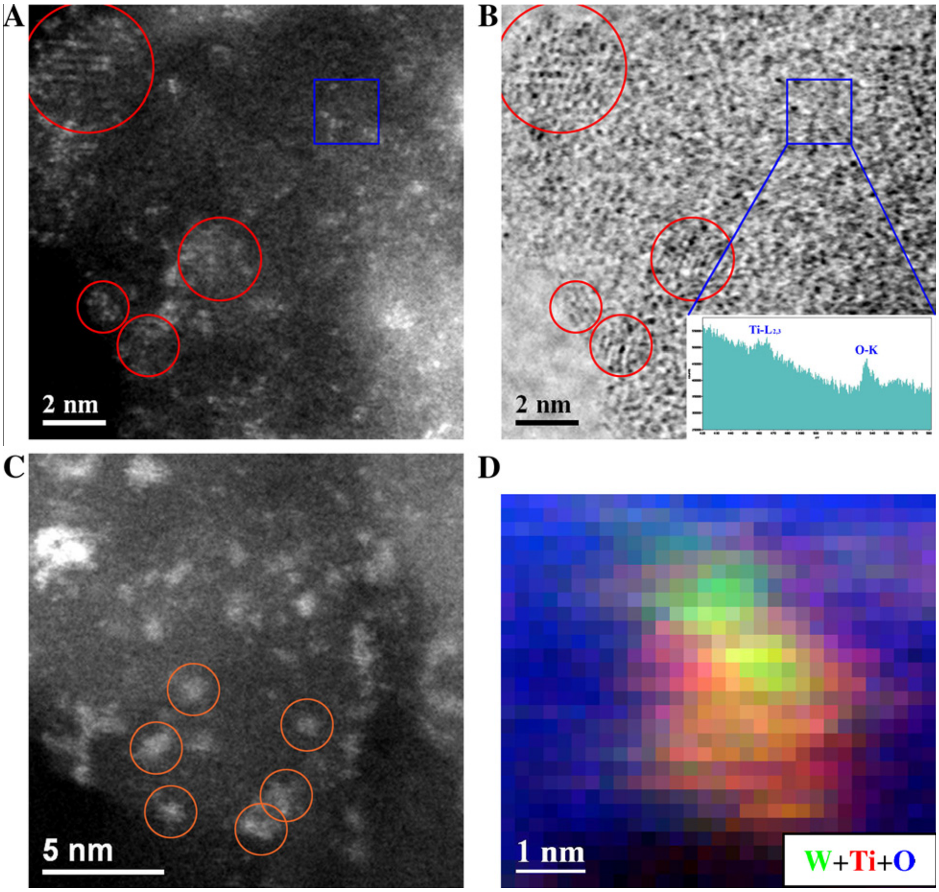

Fig. 11. (A and B) Representative pairs of HAADF (A) and BF-STEM (B) images from a $5\%WO_3/30\%TiO_2/SiO_2$ sample, which exhibited low catalytic activity; *inset:* a STEM-EELS spectrum collected from the area indicated by the square boxes in (A) and (B) showing weak Ti signals: (C and D) Representative HAADF image (C) and a reconstructed elemental distribution (D, HAADF signal in green, Ti $L_{2,3}$ EELS signal in red, and oxygen K edge EELS signal in blue) from the $5\%WO_3/5\%TiO_2/SiO_2$ sample, which exhibited a high catalytic activity. Reprinted from Ref. [63].

more sophisticated microscopy techniques will undoubtedly open up exciting opportunities for heterogeneous catalysis researchers to uncover old mysteries and make new discoveries. Here we describe a few specific technological advances that and would lead to further advances in oxide-on-oxide catalyst research.

3.1. In-situ characterization of highly dispersed catalysts by electron microscopy

It has been well documented that the catalytic activity of heterogeneous catalysts depends on the size, shape, nanostructure, and composition of the active species. It has also been shown that these key parameters can change under reaction conditions, which usually involve elevated temperature and a gaseous reaction environment. In order to better understand the relationship between the catalytic performance and the catalyst structure, information regarding the dynamic structural evolution during catalyst synthesis, catalytic reaction, and catalyst regeneration becomes important.

A critical part in an *in situ* electron microscopy experiment is the environmental gas phase reaction cell, which allows one to introduce a reactive gas into the microscope chamber around the sample without breaking the vacuum condition in the rest of the microscope. Heating capability is also required for the sample holder. Two different approaches are usually adapted. The first design requires some major modification to the microscope, and relies on a set of specially designed objective polepieces and a differential pumping system to maintain different vacuum levels around the sample stage and the rest of the microscope column. Reaction gas pressures of up to 50 mbar (5 kPa) and heating temperatures up to 1000 °C can be obtained using this design [64]. An alternative approach, as shown in Fig. 12, uses two electron-transparent ceramic membranes to isolate an ultra-thin gas layer in a differentially pumped sample grid arrangement, which would allow a gas pressure up to one atmosphere [65] and even the use of liquid reactant [66] in the microscope.

Most of the *in situ* electron microscopy studies under gaseous reaction condition environments that have been reported use TEM mode in order to minimize the effects of extra electron scattering by the reactive gas molecules. Many atomic resolution *in situ* HRTEM studies of catalysts under a few mbar pressure of gas have been reported [68], which have provided unprecedented insights into the dynamic structural evolution of catalyst particles under reaction conditions. For example, Hansen et al. [68] employed *in situ* HRTEM and observed that Cu nanocrystals on different supports undergo dynamic reversible shape changes in response to changes in the gaseous environment, which suggests that nanoparticle dynamics should be included in any description of the catalytic performance of these supported Cu catalysts. However, since TEM imaging is not the ideal technique to probe oxide species supported on oxide surfaces, *in situ* STEM experiments become an important requirement for the study of many practical catalysts involving highly dispersed surface species. Currently, *in situ* STEM experiments under reaction gas condition have rarely been reported due to the scattering between the focused electron probe and the reaction gases, which degrades the imaging resolution considerably and causes serious carbon contamination on the sample. One particularly notable piece of technical progress is that by de Jong et al. [65] recently demonstrating that ~1 nm HAADF imaging resolution can be achieved under atmospheric pressure conditions using a reaction cell design similar to that shown in Fig. 12. Although single atom detection has not yet been reported for *in situ* TEM or STEM studies under a gas environment, we expect that this may be achieved in the near future by combining the latest aberration-corrected STEM technology with an improved *in situ* cell design. Such a combination could, in principle, be used to monitor the dynamic structural evolution of highly dispersed, active sub-nm surface species during catalytic reactions, thus, providing an unprecedented view of how catalysts really change on the atomic scale.

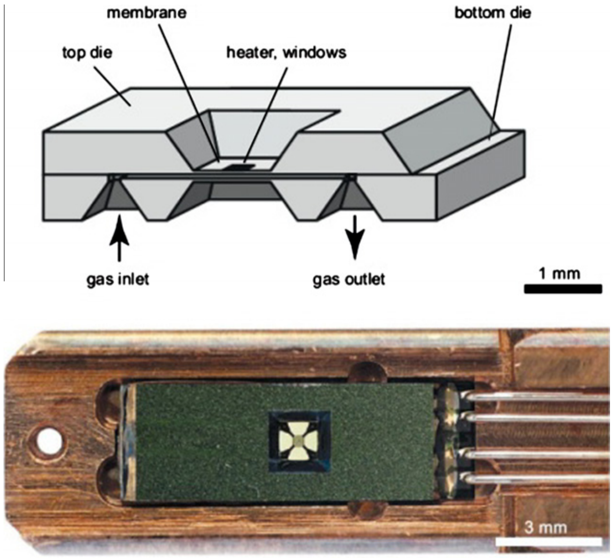

Fig. 12. Schematic diagram and photograph of a sample holder with a MEMS-based reaction cell for *in situ* (S)TEM study (Reprinted from Ref. [67] with permission from Elsevier).

Along the line of *in situ* experiments under gaseous reaction conditions, "*semi-in situ*" electron microscopy experiments involving some kind of heat treatment procedures under vacuum can also provide invaluable information on catalyst behavior at elevated temperature. Some very elegant work has recently been reported by Allard and co-workers [69], who used ProtoChips heating holders in an aberration-corrected STEM, to evaluate the thermal stability of highly dispersed noble metal species (*i.e.* Au and Pt) on various surfaces. Such *in situ* atomic resolution STEM imaging experiments, with single atom sensitivity, can provide valuable insights into the degradation mechanisms at play within a catalyst system.

Both *in situ* and "*semi-in situ*" aberration-corrected STEM characterization could have a significant impact on research into oxide-on-oxide catalysts. Take supported WO_3/ZrO_2 catalysts as an example. Time-dependent STEM imaging could be performed during an *in situ* calcination process or under reaction conditions. The *in situ* calcination experiment might help us to understand the dynamic processes involved in the formation of the catalytically active species (*i.e.* mixed Zr–WO_x clusters) from the oxide precursors and, in principle, would enable us to refine the synthesis routine. By monitoring any dynamic structural change occurring to the active surface WO_x species under reaction conditions, new insights into the induction mechanism (commonly observed in catalytic alkane isomerization reactions, see Ref. [61]) and deactivation mechanism can be obtained. New information on these important aspects can ultimately lead to a better understanding of the structure–activity relationships and help us to design better catalysts. Some of these *in situ* experiments are currently underway in our group.

3.2. Electron beam damage and gentle electron microscopy

As mentioned previously, electron beam damage is an important issue to consider for all electron microscopy studies. A general discussion of electron beam damage can be found in many electron

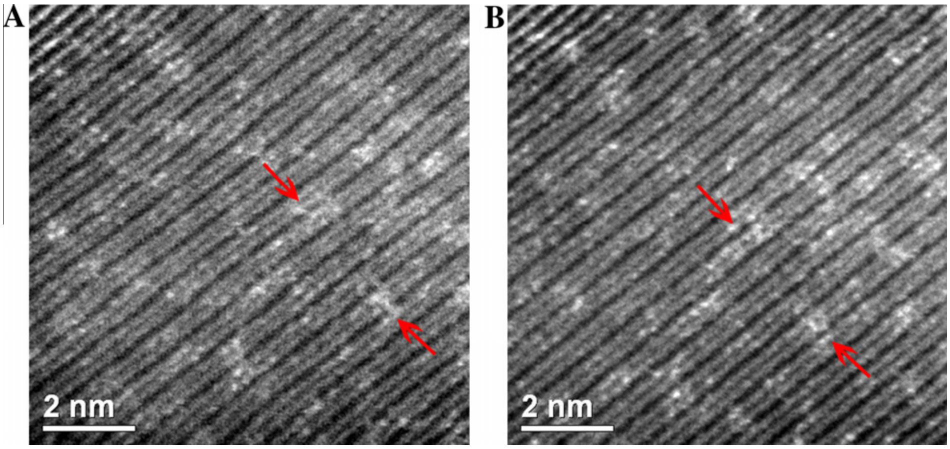

Fig. 13. Sequentially obtained STEM-HAADF images illustrating the effects of electron beam irradiation on the supported tungstate species in a low activity WO_3/ZrO_2 sample. Although the supported mono- and poly-tungstate species show some evidence of surface mobility in these two sequential images, they have no great tendency to agglomerate into clusters. These structures can persist for several minutes of continuous scanning under the experimental conditions employed (*i.e.* 200 keV, 30 pA, 48 s/pixel). Identical points in the two images are marked by arrows. Reprinted from Ref. [11].

microscopy textbooks [70] and an excellent review paper by Egerton et al. [71]. For supported oxide-on-oxide catalyst systems, the high dispersion of the surface oxide species makes it particularly challenging to acquire reliable structural information without significant beam damage.

By simply taking sequential images from the same area of the catalyst material, one can usually observe the diffusion of surface atoms induced by the electron beam. Such sequential images provide important criteria to evaluate the reliability of the structural information obtained from electron microscopy studies and for the selection of experimental conditions. Generally speaking, in order to reduce electron beam irradiation damage to the sample during imaging and analysis, one can start with a low electron dose setting (*i.e.* low electron probe current and short dwell time), and increase the electron dose step-by-step. By monitoring any structural changes of the material in sequential images taken under different electron doses, one can deduce out how long the structural integrity can be retained under each experimental condition. Usually, using low electron dose setting allows experiments to be performed on the materials for a longer period of time without significant beam damage, however, at the price of a low signal-to-noise ratio in the experimental data. In some very electron beam sensitive oxide systems, *e.g.* zeolitic materials, extremely low dose settings are required, and image processing is essential in order to extract detailed structural information from the experimental images [72]. When combined with dynamic image simulation, detailed structural evolution at the atomic scale can sometimes be clearly revealed from such sequential images [73]. It should be noted that for most supported catalyst materials, some degree of surface diffusion of surface atoms cannot be avoided during electron microscopy characterization. As long as the structures shown in sequential images are statistically the same, they can be considered as a "true" representation of the real structure in the material. An example of this is shown in Fig. 13 for the case of WO_3/ZrO_2 catalysts.

In order to reduce electron beam irradiation damage to the sample, especially direct "knock-on" damage that is prevalent in materials containing light atoms such as B, C, N and O, there is currently considerable interest in operating the electron microscope at low accelerating voltages [29,74,75]. With the very latest design of electron optics, atomic resolution HAADF imaging and EELS SI capabilities have already been demonstrated on an aberration-corrected STEM operating at 60 kV [29,74,75]. This new development now allows many catalysts, such as carbon nanotube supported catalysts or graphene supported catalysts and SiO_2-based catalysts, which suffer beam damage at conventional accelerating voltages, to be studied at atomic scale at low kV. However, it should also be noted that there are two distinct types of radiation damage possible in a sample held under an electron beam. While the knock-on damage, *i.e.* the direct displacement of atoms from the sample, can be reduced by using a low kV electron beam; the radiolysis effect, *i.e.* chemical bond breaking via inelastic scattering and ionization, becomes more severe at low kV. Therefore, the choice of operating voltage of the instrument depends on the major damage mechanism of the specific sample of interest.

4. Concluding remarks

In this review article, we have described some recent progress from our own research in the study of supported metal oxide catalysts using aberration-corrected STEM imaging and associated chemical analysis techniques. We have demonstrated that the unprecedented spatial resolution of these techniques can provide new structural views of the oxide overlayer species, help us to identify the catalytic active sites of most importance, and allow us to develop meaningful structure–activity relationships for supported oxide catalyst systems. The rapid developments that are taking place now in the areas of *in situ* microscopy and low voltage microscopy will undoubtedly open up even more opportunities to explore a wider variety of oxide based catalyst materials under working conditions.

While one can enjoy the improved resolution and sensitivity from aberration-corrected STEM imaging and chemical analysis, it should be noted that catalysts are usually structurally inhomogeneous in nature. Therefore, special attention must be paid to make sure that the local structural information obtained from localized STEM analysis is representative of the sample as a whole, *i.e.* random sampling of a large number of areas is essential. Moreover, it is advised that the local high spatial resolution structural and chemical information obtained from aberration-corrected electron microscopy characterization should be combined with information from optical spectroscopy analysis (Raman, IR and UV–vis), low energy ion scattering (LEIS) from the outermost surface layer and conventional X-ray and TEM/SEM characterization, which provide information from a larger volume of the catalyst sample. *In-situ* optical spectroscopy methods [5], in particular, can also provide complementary information on electronic structure, surface adsorbed species and bonding configuration, which cannot be easily accessed by electron microscopy methods. The combination of multiple characterization methods can provide a wider view of the oxide-on-oxide catalyst system from the macroscopic scale down to the atomic scale, and when combined with catalytic activity testing, the relationship between the structure and catalytic activity can potentially be satisfactorily deduced.

With the rapid development of high performance computing techniques, it is now becoming routine to perform atomistic simulations based on the detailed atomic scale structural and chemical information gleaned from aberration-corrected electron microscopy experiments. Such simulations, including density functional theory (DFT) calculations, can help us to better understand the relationship between the observed structure and catalytic performance. One successful example of this approach has very recently been reported in the study of the supported WO_3/ZrO_2 catalyst system [76]. It is, therefore, our belief that aberration-corrected STEM, combined with other characterization techniques and atomistic simulations, will continue to assist catalysis researchers in making new and significant discoveries in the field of oxide-on-oxide catalysts.

Acknowledgements

We would like to express our most sincere acknowledgment to our collaborators: E.I. Ross-Medgaarden, K.F. Doura, M.S. Wong, N. Soultanidis, W.V. Knowles, A.A. Herzing, G.J. Hutchings, E. Okunishi, and M. Watanabe. We thank N. Soultanidis at Rice University for his help in preparing Fig. 7. This research was sponsored by the National Science Foundation's Nanoscale Interdisciplinary Research Team (NSF-NIRT) program under grant #0609018.

References

[1] Weber RS. Effect of local-structure on the UV-Visible absorption edges of molybdenum oxide clusters and supported molybdenum oxides. J Catal 1995;151:470–4.
[2] Ross-Medgaarden EI, Wachs IE. Structural determination of bulk and surface tungsten oxides with UV-vis diffuse reflectance spectroscopy and Raman spectroscopy. J Phys Chem C 2007;111:15089–99.
[3] Ross-Medgaarden EI et al. New insights into the nature of the acidic catalytic active sites present in ZrO_2-supported tungsten oxide catalysts. J Catal 2008;256:108–25.
[4] Wachs IE. Raman and IR studies of surface metal oxide species on oxide supports: supported metal oxide catalysts. Catal Today 1996;27:437–55.
[5] Haw JF, editor. In-Situ Spectroscopy in heterogeneous catalysis. Weinheim: Wiley VCH; 2002.
[6] Herzing AA, Kiely CJ, Carley AF, Landon P, Hutchings GJ. Identification of active gold nanoclusters on iron oxide supports for CO oxidation. Science 2008;321:1331–5.
[7] Rose H. Outline of a spherically corrected semiaplanatic medium-voltage transmission electron microscope. Optik 1990;85:19–24.
[8] Krivanek OL, Dellby N, Lupini AR. Towards sub-angstrom electron beams. Ultramicroscopy 1999;78:1–11.
[9] Varela M et al. Materials characterization in the aberration-corrected scanning transmission electron microscope. Annu Rev Mater Res 2005;35:539–69.
[10] Liu JY. Scanning transmission electron microscopy and its application to the study of nanoparticles and nanoparticle systems. J Electron Microsc 2005;54:251–78.
[11] Zhou W et al. Identification of active Zr–WO_x clusters on ZrO_2 support for solid acid catalysts. Nat Chem 2009;1:722–8.
[12] Routray K, Zhou W, Kiely CJ, Grünert W, Wachs IE. Origin of the synergistic interaction between bulk metal oxide phases: selective oxidation of methanol to formaldehyde over bulk iron–molybdate catalysts. J Catal 2010;275:84–98.
[13] Haider M et al. Electron microscopy image enhanced. Nature 1998;392:768–9.
[14] Gontard LC et al. Aberration-corrected imaging of active sites on industrial catalyst nanoparticles. Angew Chem Int Edit 2007;46:3683–5.
[15] Su DS et al. Surface chemistry of Ag particles: identification of oxide species by aberration-corrected TEM and by DFT calculations. Angew Chem Int Edit 2008;47:5005–8.
[16] Okunishi E et al. Visualization of light elements at ultrahigh resolution by STEM annular bright field microscopy. Microsc Microanal 2009;15(Suppl 2):164–5.
[17] Pennycook SJ, Boatner LA. Chemically sensitive structure-imaging with a scanning transmission electron microscope. Nature 1988;336:565–7.
[18] Pennycook SJ. Z-contrast STEM for materials science. Ultramicroscopy 1989;30:58–69.
[19] Muller DA et al. Atomic-scale chemical imaging of composition and bonding by aberration-corrected microscopy. Science 2008;319:1073–6.
[20] Thomas JM, Midgley PA. The merits of static and dynamic high-resolution electron microscopy (HREM) for the study of solid catalysts. ChemCatChem 2010;2:783–98.
[21] Watanabe M et al. The aberration corrected JEOL JEM-2200FS FEG-STEM/TEM fitted with an Ω electron energy-filter: performance characterization and selected applications. JEOL News 2006;41:2–7.
[22] Erni R, Rossell MD, Kisielowski C, Dahmen U. Atomic-resolution imaging with a sub-50-pm electron probe. Phys Rev Lett 2009;102:096101.
[23] Nellist PD, Pennycook SJ. Direct imaging of the atomic configuration of ultradispersed catalysts. Science 1996;274:413–5.
[24] Voyles PM, Muller DA, Grazul JL, Citrin PH, Gossmann HJL. Atomic-scale imaging of individual dopant atoms and clusters in highly n-type bulk Si. Nature 2002;416:826–9.
[25] Scherzer O. Sphärische und chromatische Korrektur von Elektronenlinsen. Optik 1947;2:114–32.
[26] Kisielowski C et al. Detection of single atoms and buried defects in three dimensions by aberration-corrected electron microscope with 0.5-Å information limit. Microsc Microanal 2008;14:469–77.
[27] Sawada H et al. STEM imaging of 47-pm-separated atomic columns by a spherical aberration-corrected electron microscope with a 300-kV cold field emission gun. J Electron Microsc 2009;58:357–61.
[28] Wang S et al. Dopants adsorbed as single atoms prevent degradation of catalysts. Nat Mater 2004;3:143–6.
[29] Krivanek OL et al. Atom-by-atom structural and chemical analysis by annular dark-field electron microscopy. Nature 2010;464:571–4.
[30] Borisevich AY et al. Single-atom sensitivity for solving catalysis problems. Microsc Microanal 2004;10:460–1.
[31] Li ZY et al. Three-dimensional atomic-scale structure of size-selected gold nanoclusters. Nature 2008;451:46–8.
[32] Hillyard S, Silcox J. Detector geometry, thermal diffuse scattering and strain effects in ADF STEM imaging. Ultramicroscopy 1995;58:6–17.
[33] Yu Z, Muller DA, Silcox J. Effects of specimen tilt in ADF-STEM imaging of a-Si/c-Si interfaces. Ultramicroscopy 2008;108:494–501.
[34] LeBeau JM, Findlay SD, Allen LJ, Stemmer S. Quantitative atomic resolution scanning transmission electron microscopy. Phys Rev Lett 2008;100:206101.
[35] Sohlberg K, Rashkeev S, Borisevich AY, Pennycook SJ, Pantelides ST. Origin of anomalous Pt–Pt distances in the Pt/alumina catalytic system. ChemPhysChem 2004;5:1893–7.
[36] Borisevich AY, Lupini AR, Pennycook SJ. Depth sectioning with the aberration-corrected scanning transmission electron microscope. Proc Natl Acad Sci USA 2006;103:3044–8.
[37] Xin HL, Intaraprasonk V, Muller DA. Depth sectioning of individual dopant atoms with aberration-corrected scanning transmission electron microscopy. Appl Phys Lett 2008;92:013125.
[38] van Benthem K et al. Three-dimensional imaging of individual hafnium atoms inside a semiconductor device. Appl Phys Lett 2005;87:034104.
[39] Midgley PA, Ward EPW, Hungria AB, Thomas JM. Nanotomography in the chemical, biological and materials sciences. Chem Soc Rev 2007;36:1477–94.
[40] Jeanguillaume C, Colliex C. Spectrum-image: the next step in EELS digital acquisition and processing. Ultramicroscopy 1989;28:252–7.
[41] Hunt JA, Williams DB. Electron energy-loss spectrum-imaging. Ultramicroscopy 1991;38:47–73.
[42] Herzing AA et al. Energy dispersive X-ray spectroscopy of bimetallic nanoparticles in an aberration corrected scanning transmission electron microscope. Faraday Discuss 2008;138:337–51.
[43] Muller DA. Structure and bonding at the atomic scale by scanning transmission electron microscopy. Nat Mater 2009;8:263–70.
[44] Varela M et al. Spectroscopic imaging of single atoms within a bulk solid. Phys Rev Lett 2004;92:095502.
[45] Watanabe M et al. Improvements in the X-ray analytical capabilities of a scanning transmission electron microscope by spherical-aberration correction. Microsc Microanal 2006;12:515–26.
[46] Watanabe M, Okunishi E, Ishizuka K. Analysis of spectrum-imaging datasets in atomic-resolution electron microscopy. Microsc Anal 2009;23:5–7.
[47] Keenan MR, Kotula PG. Accounting for Poisson noise in the multivariate analysis of ToF-SIMS spectrum images. Surf Interface Anal 2004;36:203–12.
[48] Herzing AA, Carley AF, Edwards JK, Hutchings GJ, Kiely CJ. Microstructural development and catalytic performance of Au–Pd nanoparticles on Al_2O_3 supports: the effect of heat treatment temperature and atmosphere. Chem Mater 2008;20:1492–501.
[49] Enache DI et al. Solvent-free oxidation of primary alcohols to aldehydes using Au–Pd/TiO_2 catalysts. Science 2006;311:362–5.
[50] Edwards JK et al. Switching off hydrogen peroxide hydrogenation in the direct synthesis process. Science 2009;323:1037–41.
[51] Burrows A, Kiely CJ, Joyner RW, Knozinger HK, Lange F. An HREM study of the WO_3/TiO_2monolayer catalyst system. Proposals for the overlayer structure. Catal Lett 1996;39:219–31.
[52] Satsuma A et al. Direct observation of polytungstate cluster and monolayer tungstate on zirconium oxide by high-resolution TEM. Chem Lett 2004;33:1250–1.
[53] Cortés-Jácome MA, Angeles-Chavez C, Bokhimi X, Toledo-Antonio JA. Generation of WO_3–ZrO_2 catalysts from solid solutions of tungsten in zirconia. J Solid State Chem 2006;179:2663–73.

[54] Cortés-Jácome MA et al. Migration and oxidation of tungsten species at the origin of acidity and catalytic activity on WO_3–ZrO_2 catalysts. Appl Catal A-Gen 2007;318:178–89.

[55] Routray K, Zhou W, Kiely CJ, Wachs IE. Catalysis science of methanol oxidation over iron vanadate catalysts: nature of the catalytic active sites. ACS Catal 2011;1:54–66.

[56] Kim T, Burrows A, Kiely CJ, Wachs IE. Molecular/electronic structure-surface acidity relationships of model-supported tungsten oxide catalysts. J Catal 2007;246:370–81.

[57] Zhou W. Nanostructural and chemical characterization of supported metal oxide catalysts by aberration corrected analytical electron microscopy. PhD thesis, Lehigh University; 2011.

[58] Borisevich AY et al. Dual nanoparticle/substrate control of catalytic dehydrogenation. Adv Mater 2007;19:2129–33.

[59] Cortes-Jácome MA et al. WO_x/TiO_2 catalysts via titania nanotubes for the oxidation of dibenzothiophene. Chem Mater 2007;19:6605–14.

[60] Pennycook SJ, Varela M, Lupini AR, Oxley MP, Chisholm MF. Atomic-resolution spectroscopic imaging: past, present and future. J Electron Microsc 2009;58:87–97.

[61] Soultanidis N et al. Relating pentane isomerization activity to the acidic properties and surface density of WO_x/ZrO_2. J Am Chem Soc 2010;132:13462–71.

[62] Ross-Medgaarden EI et al. Tuning the electronic and molecular structures of catalytic active sites with titania nanoligands. J Am Chem Soc 2009;131:680–7.

[63] Zhou W et al. Aberration-corrected analytical microscopy characterization of double-supported WO_3 /TiO_2 /SiO_2 solid acid catalysts. ChemCatChem 2011;3:1045–50.

[64] Davis RJ et al. In: WTEC Panel Report on International Assessment of Research and Development in Catalysis by Nanostructured Materials. Baltimore: World Technology Evaluation Center Inc.; 2009.

[65] de Jonge N, Bigelow WC, Veith GM. Atmospheric pressure scanning transmission electron microscopy. Nano Lett 2010;10:1028–31.

[66] de Jonge N, Peckys DB, Kremers GJ, Piston DW. Electron microscopy of whole cells in liquid with nanometer resolution. Proc Natl Acad Sci USA 2009;106:2159–64.

[67] Creemer JF et al. Atomic-scale electron microscopy at ambient pressure. Ultramicroscopy 2008;108:993–8.

[68] Hansen PL et al. Atom-resolved imaging of dynamic shape changes in supported copper nanocrystals. Science 2002;295:2053–5.

[69] Allard LF et al. Evolution of gold structure during thermal treatment of Au/FeO_x catalysts revealed by aberration-corrected electron microscopy. J Electron Microsc 2009;58:199–212.

[70] Williams DB, Carter CB. Transmission electron microscopy: a textbook for materials science. New York: Springer; 2009.

[71] Egerton RF, Li P, Malac M. Radiation damage in the TEM and SEM. Micron 2004;35:399–409.

[72] Ortalan V, Uzun A, Gates BC, Browning ND. Direct imaging of single metal atoms and clusters in the pores of dealuminated HY zeolite. Nat Nanotechnol 2010;5:506–10.

[73] Ortalan V, Uzun A, Gates BC, Browning ND. Towards full-structure determination of bimetallic nanoparticles with an aberration-corrected electron microscope. Nat Nanotechnol 2010;5:843–7.

[74] Suenaga K et al. Visualizing and identifying single atoms using electron energy-loss spectroscopy with low accelerating voltage. Nat Chem 2009;1:415–8.

[75] Krivanek OL et al. Gentle STEM: ADF imaging and EELS at low primary energies. Ultramicroscopy 2010;110:935–45.

[76] Xu H, Neurock M. First principles analysis of methanol dehydration over tungstated zirconia. 2010 AIChE Annual Meeting; 2010.